NJC

ROYAL SOCIETY OF CHEMISTRY

PAPER

View Article Online
View Journal | View Issue

Cite this: *New J. Chem.*, 2021, 45, 6486

Supramolecular kinetic effects by pillararenes: the synergism between spatiotemporal and preorganization concepts in decarboxylation reactions†

Eduardo Vieira Silveira, *[a] Rodrigo Montecinos, [b] Leandro Scorsin,[a] Luis Garcia-Rio, *[c] Michelle Medeiros,[a] Vanessa Nascimento, [d] Faruk Nome,‡[a] Ricardo F. Affeldt [a] and Gustavo A. Micke[a]

A study about spontaneous decarboxylation reactions of 3-carboxy-1,2-benzisoxazole (CBI) nitrated derivatives (6-NitroCBI and 5,6-DinitroCBI) compared with supramolecular kinetic effects promoted by two cationic pillararenes (P5A and P6A) has been carried out and brings contributions to advance current theories related to supramolecular and enzymatic catalysis/inhibition. A higher energy barrier to spontaneous hydrolysis of 6-NitroCBI relative to that of 5,6-DinitroCBI ($\Delta\Delta G^{\ddagger}$ = 2.98 kcal mol^{-1}) was determined experimentally, however similar transitions states were observed for both substrates. The host–guest complexes generated catalytic effects up to 7.1-fold on k_{obs}, except for 6-NitroCBI⊂P5A which is the only system that presented unprecedent inhibitory kinetic effects. The data (kinetics, ^{1}H NMR titration and molecular dynamic simulations) elucidated the kinetic effects of the four complexes as a result of their geometries, more specifically, by modifying 3 main factors: (1) number of hydrogen bonds between solvent and carboxyl groups of the CBIs, (2) polarization of the O–N bond of the isoxazole ring and (3) reduction of the inductive effect of NO_2 groups by field effects. The data from the present study encourage the use of both spatiotemporal and preorganization theories during interpretations related to supramolecular and enzymatic catalysis.

Received 2nd February 2021,
Accepted 17th March 2021

DOI: 10.1039/d1nj00551k

rsc.li/njc

1. Introduction

Research groups of different areas and distinct ideologies search for the elucidation of enzymatic catalytic effects. However, these developed studies provided a discussion between two very well-founded theories committed to solving these fundamental questions, both always presenting valid arguments and evidences. On the one hand,[1,2] spatiotemporal theory postulates that such effects occur from an ideal proximity (~3 Å) and rigidity (or length time) between reactive groups, factors that are experimentally determinable and controllable. By the other side,[3] the effects in preorganization theory can be briefly described by the large free-energy penalty already paid by preorganized dipoles (commonly represented theoretically by water molecules) at the enzymatic active site. Despite studies of vibrational Stark effect spectroscopy already carried out on enzymes,[4–6] the lack of technology to investigate these fundamental issues can be supplied by supramolecular chemistry using smaller and simpler mimetic structures.

Supramolecular chemistry shows high potential to solve fundamental and practical issues related to different areas. The remarkable characteristics of self-assembly control and generation of particular chemical environments with high affinity for different classes of substrates offer fundamental conditions to investigate and mimic natural biological structures.[7,8] These characteristics are observed in several supramolecular systems such as by the use of different macrocycles to host–guest (H:G) complexation. For this purpose, pillararenes represent a recent class of macrocycles with versatility already proven by the diverse studies related to catalysis,[9,10] analytical,[11,12] environmental,[13] food,[14,15] materials,[16,17] therapeutic/medical[18,19] and among others. Furthermore, some studies suggest that the investigation of pillararenes

[a] *Department of Chemistry, Federal University of Santa Catarina, Florianópolis, SC, 88040-900, Brazil. E-mail: eduardovieira.chem@gmail.com*
[b] *Faculdad de Química, Pontificia Universidad Católica de Chile, Av. Vicuña Mackenna 4860, Santiago, Chile*
[c] *Departamento de Química Física, Centro de Investigación en Química Biolóxica e Materiais Moleculares (CIQUS), Universidade de Santiago de Compostela, 15782 Santiago de Compostela, Spain*
[d] *Department of Organic Chemistry, Fluminense Federal University, Niterói, RJ, 24020-150, Brazil*

† Electronic supplementary information (ESI) available. See DOI: 10.1039/d1nj00551k

‡ Dr. Faruk Nome passed away on September 24, 2018.

may assist in the understanding of larger biological systems and their natural processes, for example, the catalytic effects promoted by enzymes.[9,10] This idea can be experimentally carried out in different ways including the use of sensitive kinetic probes such as the 3-carboxy-1,2-benzisoxazole (CBI) and its derivatives.[20]

The 3-substituted-1,2-benzisoxazoles have been described as a promising class of heterocycle with significant biological activities,[21–25] commonly associated with serotonergic and dopaminergic receptors.[26] Belonging to this class, CBI is an organic acid that has its decarboxylation reaction well studied in aqueous and organic media,[20,27–29] in the presence of surfactants/premicelles,[30] antibody and albumin,[31] cationic polymer,[32] micelles,[33] vesicles[34] and quaternary ammonium macrocycles.[35] Some particularities are notable for this reaction like the high sensitivity to its ionization state (favored as carboxylate), polarity of the medium (favored by polar solvents) and number of hydrogen bonds (HBs) between its COO^- group and solvent (favored by aprotic solvents), reaching up to 10^8-fold increases on k_{obs}.[28] This high kinetic sensitivity allows us to propose the use of CBI and its derivatives as potential probes to investigate the properties of chemical environments offered by hosts by monitoring changes in k_{obs}. Through theses studies important information may potentially be able to collaborate with the spatiotemporal *vs.* preorganization discussion.

Here we describe an experimental and theoretical study about spontaneous decarboxylation reactions of 6-NitroCBI (6-nitro-1,2-benzisoxazole-3-carboxylic acid, Chart 1) and 5,6-DinitroCBI (5,6-dinitro-1,2-benzisoxazole-3-carboxylic acid, Chart 1) compared with supramolecular kinetic effects promoted by two cationic pillar[*n*]arenes (*n* = 5 or 6) functionalized with trimethylammonium groups (P5A and P6A, Chart 1). The experiments in pure water (buffered when described) and in the presence of pillararenes provided relevant information about CBI derivatives both individually and when in complexes. Kinetics, ^{1}H NMR titration and molecular dynamics simulations are consistent with H:G stoichiometry, the cavity size of macrocycles influencing the kinetic effect type (catalysis or inhibition, unprecedented for the latter) as well as the magnitude of binding ($K_{1:1}$) and rate constants ($k_{1:1}$). The kinetic effects observed in these enzyme mimics could not be explained with just one of the theories under discussion (spatiotemporal or preorganization), but when both were considered simultaneously.

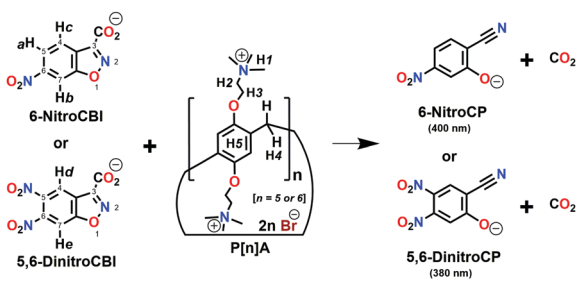

Chart 1 Decarboxylation reactions of the 6-NitroCBI or 5,6-DinitroCBI in the presence of the P5A or P6A to form the corresponding cyanophenolates (CPs) and carbon dioxide.

2. Experimental

2.1 Materials

The CBI derivatives and pillararenes were prepared on the basis of the literature,[28–45] with the modifications detailed in the ESI.†

2.2 Kinetics

Reactions were followed with an UV-Vis spectrophotometer equipped with a Peltier temperature controller set at 25.0 °C, except to obtain the thermodynamic parameters, in which case the temperature was varied between 25–65 °C. Reactions were started by adding 20.0 μL of a CBI solution at 0.01 mol L^{-1} (in acetonitrile) to 2.0 mL of buffer solution in quartz cuvettes, in the presence or absence of the pillararenes. All k_{obs} were measured by the appearance of the 5,6-DinitroCP or 6-NitroCP at 380 and 400 nm, respectively. Except for the pH-rate profile, the reactions were performed at pH 7.0 ([Bis–Tris methane] = 0.01 mol L^{-1}).

2.3 ESI-MS

CBIs were solubilized in acetonitrile (~10 μM) and decarboxylation induced by sonication and heating, the expected *m*/*z* values being confirmed for both CBIs. The samples were injected directly to a mass spectrometry system consisting of a hybrid triple quadrupole/linear ion trap mass spectrometer Q trap 3200 (Applied Biosystems/MDS Sciex, Concord, Canada). The experiments were performed using the Turbo Ion Spray™ source (electrospray ionization-ESI, Applied Biosystems/MDS Sciex, Concord, Canada) in negative ion mode. Samples were infused continuously at 10 μL min^{-1} with a syringe pump. The capillary needle voltage was maintained at −4.5 kV. The MS/MS parameters were curtain gas, 18 psi; ion spray interface, 400 °C; gas 1 : 45 psi; gas 2 : 45 psi; and collision gas, medium.

2.4 NMR

For product characterization, CBIs were solubilized in acetone-D_6 and decarboxylation induced by sonication and heating. The structures were confirmed by ^{1}H and ^{13}C{^{1}H} analysis using a Bruker AC 200 MHz spectrometer. For ^{1}H NMR titrations, to the NMR tube containing the CBI derivative were added solid fractions of the pillararene and after total solubilization of each addition the spectrum was collected.

2.5 Intrinsic reactions coordinates

Density Functional Theory (DFT) calculations were performed at the M06[46]/6-31+G(d,p) level of theory using GAUSSIAN 09 package.[47] The default parameters for convergence, *viz.* the Berny analytical gradient optimization routine were used; convergence on the density matrix was 10^{-9} atomic units, the threshold value for maximum displacement was 0.0018 Å, and the maximum force 0.00045 hartree $bohr^{-1}$. All optimizations and frequency calculations were performed using the Polarizable Continuum Model (PCM) and the Solvation Model Density (SMD) of Truhlar and coworkers.[48] The transition states (TS, Fig. S11-b, ESI†) were identified by their single imaginary frequencies.

2.6 Molecular dynamics simulations

Simulations were performed using the program package Gromacs version 4.6.5.[49] Pillararenes and CBI derivatives were built with parameters from the GROMOS96 54A7[50] force field and solvated with the SPC water model.[51] Periodic boundary conditions were applied in all three dimensions. All simulations were carried out in the isothermal–isobaric ensemble. The temperature was maintained at 300 K using the Berendsen thermostat (v-rescale) with pillararenes and CBI derivatives, and ions and water coupled independently, with a coupling time constant of 0.1 ps. The pressure was maintained at 1 bar using the Berendsen barostat with a coupling time constant of 1.0 ps.[52] The LINCS algorithm was used to constrain the bond lengths of the pillararenes and CBI derivatives and SETTLE to restrict the structure of the water molecules. A 1.2 nm cut-off was used for the van der Waals interactions. Long-range electrostatic interactions were calculated using the particle mesh Ewald (PME).[53] A time step of 2 fs was used throughout the simulations. The neighbor list was updated every 10 time steps. Both systems were equilibrated by 500 ps. Trajectories of 20 ns were calculated for each system. To explore the most probable structures formed by the interactions between the compounds 6-NitroCBI and 5,6-DinitroCBI with P5A and P6A, molecular dynamics simulations (MD) of the four systems were performed. Each system containing one CBI derivative and one macrocycle was solvated with 4714 water molecules (SPC) in the presence of appropriate quantities of Br^- and Na^+ to reach the electroneutrality of the system.

3. Results and discussion

3.1 Spontaneous decarboxylation reactions

A study evaluated the influence of 24 solvents on the decarboxylation reaction of the anionic 6-NitroCBI, showing that polar solvents favor the reaction by modification of electronic effects, while aprotic solvents favor by modification of hydrogen bonding (HBs, between solvent and its COO^- group).[28] These kinetic effects represent increases up to 10^8-fold in k_{obs}, making this reaction an excellent probe to investigate the properties offered by different chemical environments. Based on this particularity, firstly we studied the spontaneous decarboxylation reactions of the 6-NitroCBI and 5,6-DinitroCBI at different acetonitrile : water ratios. The results (Fig. S5 and Table S3, ESI†) showed that the rate of reaction increases exponentially by reducing the fraction of water, with increase in k_{obs} of approximately 200 and 400-fold at 75% acetonitrile for 6-NitroCBI and 5,6-DinitroCBI, respectively. These results corroborate the idea that nonpolar and protic solvents stabilize the starting material and allowed us to later compare the nanoenvironments offered by the pillararenes cavities with acetonitrile percentage.

The kinetic pK_a values (pK_{ac}) were also determined by data fitting of k_{obs} *vs.* H_0/pH graphs (Fig. S6, ESI†), presenting values of 1.61 and 1.18 for 6-NitroCBI and 5,6-DinitroCBI, respectively. NMR and ESI-MS experiments confirmed the structure of the cyanophenolates (CPs), the products of the decarboxylation reactions (Table S1 and Fig. S2–S4, ESI†). Isotope effects (k_w/k_D, Table 1) of 1.18 and 1.07 were observed to 6-NitroCBI and 5,6-DinitroCBI, respectively. These subtle isotope effects can indicate a destabilization of the TSs of the CBI derivatives during decarboxylation reactions due to the lower vibrational frequency of the O–D (oxygen–deuterium) bond. The smallest effect observed for the 5,6-DinitroCBI could be associated with the greater difference between its pK_a and the corresponding of water.[36] The experimental activation parameters were obtained for both derivatives from good Eyring relationship (Fig. S7, ESI† and Table 1), with the favoring of 5,6-DinitroCBI ($\Delta\Delta G^{\ddagger}$ = 2.98 kcal mol^{-1}) governed by the smaller enthalpy of activation, even with the half of the entropic gain when compared to 6-NitroCBI.

The computational study indicates the presence of TSs for both substrates during the decarboxylation reactions. The IRCs (Fig. S11-Above; calculated considering the optimized structure of the reagent as the starting point, ΔE = 0, ESI†) represents a total energetic variation of $\Delta\Delta E$ = 7.32 kcal mol^{-1} between both substrates as a result of a new electron withdrawing group (NO_2) added to 5-position in the benzisoxazole ring. The molecular structures of the TSs (Fig. S11-Below, ESI†) assisted by two water molecules corroborates the structures already reported for the CBI in aqueous medium,[37–40] with the bonds cleaved (represented by the arrows) presenting similar distances

Table 1 Experimental and theoretical activation parameters of spontaneous decarboxylation reactions of anionic CBI derivatives. Dihedral angles and interatomic distances for TSs of the same reactions (pH 7.00; [Bis–Tris methane] = 0.01 mol L^{-1}; M06/6-31G+(d,p) theory level)

CBI	Study	$\Delta G^{\ddagger}$ (kcal mol^{-1})	$\Delta H^{\ddagger}$ (kcal mol^{-1})	$\Delta S^{\ddagger}$ (cal mol^{-1} K^{-1})	Dihedral [C–C–C–O]	Distance C–C (Å)	Distance N–O (Å)
 6-NitroCBI	Experimental	24.98	32.42	24.95	—	—	—
	Theoretical	24.77	25.16	1.31	90.51°	1.76	2.15
 5,6-DinitroCBI	Experimental	22.00	25.34	11.23	—	—	—
	Theoretical	17.17	17.57	1.34	92.24°	1.72	2.06

$k_W/k_{D(6\text{-NitroCBI})} = 3.00 \times 10^{-6}/2.55 \times 10^{-6} = 1.18$; $k_W/k_{D(5,6\text{-DinitroCBI})} = 4.65 \times 10^{-4}/4.34 \times 10^{-4} = 1.07$.

for both CBI derivatives. Another similar evidence for the two derivatives is related to the dihedral angle [C–C–C–O], which has a torsion of approximately 90° in relation to the reagent. Corroborating with the experimental data, the higher Gibbs free energy of activation ($\Delta G^{\ddagger}$) calculated for 6-NitroCBI relative to 5,6-DinitroCBI ($\Delta\Delta G^{\ddagger}$ = 7.60 kcal mol^{-1}) is governed by the enthalpy of activation, but here the activation entropy is similar between the substrates. However, the highest calculated $\Delta\Delta G^{\ddagger}$ results from the divergence in enthalpy–entropy compensation for 5,6-DinitroCBI, which can be a result of the lower enthalpic contribution from its late TSs structure. This latter affirmation is in agreement with the smaller C–C atomic distances of its structure comparing with that already reported to CBI.[37] These information are presented in Table 1 together with their corresponding experimental data.

3.2 Kinetic effects of P5A and P6A

Substrates sensitive to different chemical environments (such as CBI derivatives) are an alternative way to investigate the properties offered by the pillararenes cavities observing the generated supramolecular kinetic effects. Based on this idea, the decarboxylation reaction of both anionic CBI derivatives were studied at pH 7.00 in the presence of P5A and P6A. The catalytic and inhibitory effects were initially expected for cavities capable of destabilizing (as observed for polar and aprotic solvents) and stabilizing (as observed for nonpolar and protic solvents) the reagents, respectively. For the treatment of the experimental kinetic data it was considered the simultaneous decarboxylation reaction in water and in the pillararene cavity, using eqn (S2) and (S3) (see ESI†) to evaluate the stoichiometry, rate and binding constants (by non-linear fitting of the curves k_{obs} *vs.* pillararene concentration).

The kinetic effects of the pillararenes (Fig. 1 and Table 2) showed modest increases on k_{obs} with increasing pillararene concentration, except for the 6-NitroCBI⊂P5A system that presented unprecedented inhibitory kinetic effect. The data fitting (Fig. 1) were satisfactory for all four systems with H:G model, this stoichiometry being confirmed for some systems by ^{1}H NMR titration.

Even though both CBI derivatives belong to the same structural class and exhibit similar sensitivity to the chemical environment, the observation of opposite kinetic effects (catalysis and inhibition) initially suggested a difference in the mode of accommodation inside the pillararenes cavities, that is, in the geometry of the complexes. In the same way, the similarity between some binding constants (or stabilization energies, ΔG) can be related to the formation of complexes of the same geometry. The similarity between the energy stabilization achieved by the complexes 6-NitroCBI⊂P6A (−22.85 kJ mol^{-1}) and 5,6-DinitroCBI⊂P6A (−22.70 kJ mol^{-1}) corroborates this idea, with P6A promoting up to 4.1 and 7.1-fold catalysis for the decarboxylation of 6-NitroCBI and 5,6-DinitroCBI, respectively. In contrast, the opposite kinetic effects and the discrepant energy stabilizations achieved by the complexes 6-NitroCBI⊂P5A (−29.13 kJ mol^{-1}) and 5,6-DinitroCBI⊂P5A (−18.88 kJ mol^{-1}) suggest different geometric structures for these complexes. These factors were initially comprised by the smaller macrocycle cavity and the additional NO_2 group in the 5-position of the benzisoxazole ring in the 5,6-DinitroCBI⊂P5A system.

The catalytic effects were preliminarily understood by the ability of the pillararenes to destabilize the CBI derivatives based on reducing the number of HBs between water and its COO^- groups. After observing the great proximity between the charged groups of the complexes (COO^- and NMe_3^+) on the molecular dynamics simulations data (MD, topic 3.4), the possibility of COO^- groups to be found in the center of the macrocycle cavity was disregarded. Thus, this reduction of HBs was not attributed to the hydrophobicity in the pillararenes cavities, but rather involves the high ability of NMe_3^+ groups to modify the water structure. To demonstrate this, the decarboxylation reactions were investigated in the presence of different tetramethylammonium bromide (TMA) concentrations in order to simulate the high concentration of NMe_3^+ groups found in the pillararenes portals. The influence of TMA on the structural properties of water is widely studied,[41–43] demonstrating that cationic TMA$^+$ presents low water concentration in its hydration layer, typical behavior of nonpolar compounds. The increase of this effect occurs with its concentration, further reducing the number of hydration water molecules and, consequently, the number of HBs between them.

Fig. S8 (ESI†) shows exponential increments on k_{obs} with TMA concentration. This observation is not related to ionic strength effects since several CBI derivatives have their reactivity unchanged up to 1 mol L^{-1} of KCl.[28] Therefore, the catalytic effects observed for 6-NitroCBI⊂P6A, 5,6-DinitroCBI⊂P5A and 5,6-DinitroCBI⊂P6A systems coincides with the spontaneous decarboxylation rate constants of the corresponding derivative at TMA concentrations of 2.02, 2.85 and 3.80 mol L^{-1}, respectively. These catalytic effects can also be correlated to the chemical environments offered by the different acetonitrile percentages, with the same sequence of the complexes corresponding to the rate constants of the spontaneous reactions at 18.9, 17.1 and 23.4% acetonitrile. An exception to this idea occurs in the 6-NitroCBI⊂P5A complex, being its inhibitory effect elucidated by NMR and MD data.

The experimental results for all systems are consistent with H:G association, where decarboxylation reaction occurs simultaneously in water and inside of the pillararene cavity.

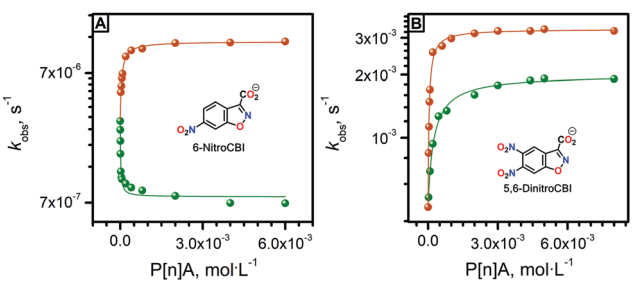

Fig. 1 Influence of (●) P5A and (●) P6A concentration on the k_{obs} for decarboxylation reactions of (A) 6-NitroCBI and (B) 5,6-DinitroCBI ([CBIs] = 1.0 × 10^{-4} mol L^{-1}; pH 7.00; [Bis–Tris methane] = 0.01 mol L^{-1}; 25.0 °C).

Table 2 Rate and binding constants of both anionic CBI derivatives in H_2O, and P5A and P6A cavities (pH 7.00; 25.0 °C)

	6-NitroCBI		5,6-DinitroCBI	
Env.	$k_{1:1}$ (s^{-1})	$K_{1:1}$ (M^{-1})	$k_{1:1}$ (s^{-1})	$K_{1:1}$ (M^{-1})
H_2O	$(3.00 \pm 0.41) \times 10^{-6}$	—	$(4.65 \pm 0.10) \times 10^{-4}$	—
P5A	$(7.77 \pm 0.53) \times 10^{-7}$	$(1.27 \pm 0.21) \times 10^{5}$ [a]	$(2.01 \pm 0.08) \times 10^{-3}$	$(2.03 \pm 0.21) \times 10^{3}$ [c]
P6A	$(1.23 \pm 0.01) \times 10^{-5}$	$(1.01 \pm 0.06) \times 10^{4}$ [b]	$(3.30 \pm 0.05) \times 10^{-3}$	$(9.49 \pm 0.70) \times 10^{3}$ [d]

[a] $\Delta G = -29.13$ kJ mol^{-1}. [b] $\Delta G = -22.85$ kJ mol^{-1}. [c] $\Delta G = -18.88$ kJ mol^{-1}. [d] $\Delta G = -22.70$ kJ mol^{-1} (calculated by $\Delta G = -R{\cdot}T{\cdot}\ln K_{1:1}$).

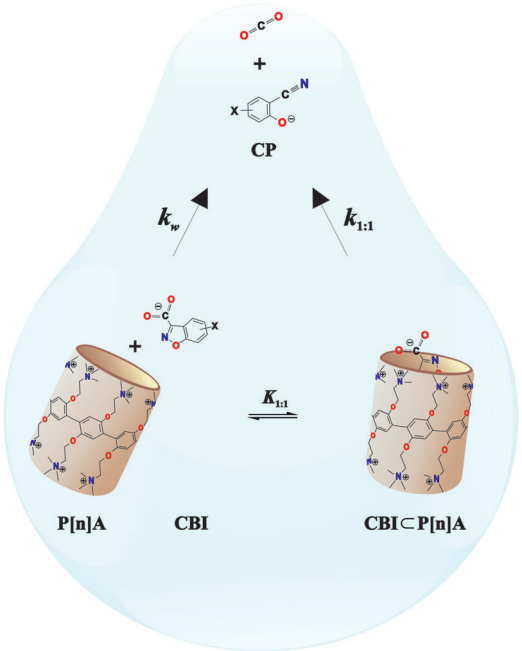

Scheme 1 General representation of the H:G association between a CBI derivative and a P[*n*]A, with decarboxylation reaction occurring in both environments (H_2O and inside of the P[*n*]A cavity).

These considerations led us to Scheme 1, which represents the generic behaviour involving kinetic and binding parameters for the four studied systems.

3.3 ^{1}H NMR titration

Usually, hydrogen signals from host and guest when in the complex present upfield or downfield shifts giving information about the system, being the ^{1}H NMR titration a powerful alternative to elucidate the stoichiometry, affinity and the structure of the complexes. The fast decarboxylation of 5,6-DinitroCBI and its catalysis by both pillararenes as well as by organic solvent fractions compromised the accuracy in obtaining the successive spectra. Thereby, the NMR data correspond only to the 6-NitroCBI⊂P5A and 6-NitroCBI⊂P6A systems using 20% of organic solvent (to solubilize the 6-NitroCBI), with the modification in the experimental conditions (relative to the kinetics) still providing relevant information about the complexes.

The successive spectra showed similar behaviours for 6-NitroCBI aromatic hydrogens in the presence of both pillararenes (Fig. S9, ESI†), with the upfield shift when in the complex indicating its accommodation in the region of greater magnetic shielding in the pillararenes cavities ($\Delta\delta_{P5A}$ = 1.26 ppm; $\Delta\delta_{P6A}$ = 0.24 ppm). We emphasize that all hydrogens from pillararenes also displayed upfield shift when in the complex without reaching a plateau, a continuous deshielding that indicates the association of Br^- with increasing pillararene concentration.[44] Another important observation is the splitting of P5A hydrogens (Fig. S9 and S10, ESI†) in the order of H2 ≫ H5 ≅ H3, a first indication of the external accommodation of the 6-NitroCBI where there is great magnetic influence on one of the P5A portals (effects not observed for its complexation with P6A).

The successive spectra also provide an experimental evidence regarding the 6-NitroCBI⊂P5A inhibitory complex. The significant shielding effect on the methylene bridge hydrogens ($\Delta\delta_{H4} \cong 0.16$, Fig. S10, ESI†) suggests the accommodation of the bulky NO_2 group in the center of the P5A cavity, a condition that would displace the high electronic density of the P5A cavity to the H4 hydrogens. These considerations suggest that kinetic inhibition could occur partially by donor field effects (by P5A arenes) on the NO_2 group, which may directly reflect the reduction of its electron withdrawing inductive effects. This is also supported by the MD data along with additional factors involved in reaction inhibition.

The data fitting of $\Delta\delta$ *vs.* pillararene concentration (Fig. 2, eqn (S4), ESI†) provided $K_{1:1}$ values of 4201 ± 1513 M^{-1} and 429.68 ± 69.76 M^{-1} for 6-NitroCBI⊂P5A and 6-NitroCBI⊂P6A, respectively. Comparing with the kinetic data, this reduction in $K_{1:1}$ (30-fold with P5A and 23-fold with P6A) suggests the hydrophobic effects as one of the main driving forces involved in the association of 6-NitroCBI with both pillararenes. In energetic terms this is represented by the loss in energy stabilizations of

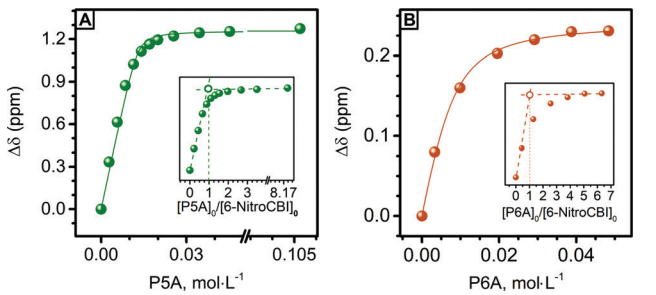

Fig. 2 ^{1}H NMR chemical shifts of the aromatic protons of 6-NitroCBI in response to the increased (A, ●) P5A and (B, ●) P6A concentration, data fitting as H:G model. The inset is the molar ratio method applied to the same data ([6-NitroCBI]$_{P5A}$ = 12.93 mmol L^{-1}; [6-NitroCBI]$_{P6A}$ = 7.65 mmol L^{-1}; D_2O : MeOD, 8 : 2, v/v; pD 7.00; 25.0 °C; 200 MHz).

$\Delta\Delta G$ = 8.45 and 7.82 kJ mol^{-1} for 6-NitroCBI⊂P5A and 6-NitroCBI⊂P6A, respectively. These data further suggest that in highly hydrophobic environments the system can act by releasing 6-NitroCBI as a result of the energy destabilization of the complexes, a perspective of great interest in the therapeutic/medicinal area mainly because several 3-substituted-1,2-benzisoxazole compounds are marketed as therapeutic drugs. The molar ratio method applied to $\Delta\delta$ *vs.* [Pillararene]$_0$/[6-NitroCBI]$_0$ (inserted in Fig. 2) has its inflection point in 1.0, what confirm the H:G binding stoichiometry for the 6-NitroCBI complexation with both pillararenes.

3.4 Molecular dynamics simulations

The most probable structures were investigated for the four complexes, all presenting the nitrobenzene region of the CBI derivatives inserted in the macrocycle cavity (Fig. 3). Accordingly with our experimental data concerning stabilization energies (Table 2), while the complexes formed with P5A presented distinct geometries, P6A has the ability to accommodate both CBIs equally. To explore these four structures as well as their stability as a function of time five parameters (*P*1–*P*5) were assessed: (*P*1) the average distance between carbon 6 (C6) from CBI derivative and the center of the pillararene cavity (CPC); (*P*2) the spatial orientation/angle of the CBI derivative in the CPC; (*P*3) the average distance between charged groups (COO^- and NMe_3^+); (*P*4) the energetic contributions resulting from electrostatic (EL) and van der Waals (VDW) interactions and (*P*5) the number of HBs between water and COO^- group from CBI derivative. All of these parameters are well discussed below and some graphics presented in ESI† (Fig. S12–S16).

The five parameters calculated for all complexes (Table 3) showed in detail some particularities of the systems and helped in understanding both catalytic and inhibitory kinetic effects promoted by the nanoenvironment offered by the pillararenes cavities. The two complexes involving the P6A have their structural similarities proven by the equivalence (*P*1, *P*2, *P*3, *P*4 and EL) or great similarity (*P*5) between parameters. Despite the same EL contributions (−100 kJ mol^{-1}), the VDW interactions were more expressive for 5,6-DinitroCBI (−205 kJ mol^{-1}) than 6-NitroCBI (−165 kJ mol^{-1}) due to the additional interactions promoted by the second NO_2 group. The smallest number of HBs (*P*5) were observed for these complexes, a parameter that confirms our experimental results and proposal for the catalytic mechanism promoted by the pillararenes, that is, reduction of HBs between COO^- group and water.

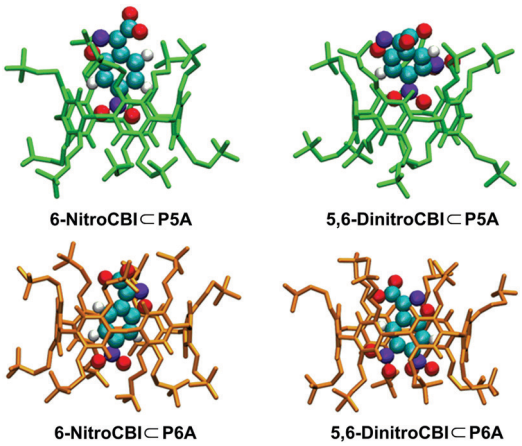

Fig. 3 Snapshots of the H:G complexes formed between CBI derivatives and cationic pillararenes. (above) External interaction of 6-NitroCBI and 5,6-DinitroCBI with P5A. (below) Deeper insertion of the 6-NitroCBI and 5,6-DinitroCBI in the P6A cavity. Pillararenes and CBI derivatives are represented in thin sticks and VDW, respectively.

In contrast, the divergence among all parameters in the complexes involving P5A can be broadly understood by its smaller cavity size and by the additional NO_2 group in one of the CBI derivative, being the steric hindrance an unfavorable and crescent phenomena in order of 6-NitroCBI⊂P5A < 5,6-DinitroCBI⊂P5A. For the latter system, the additional NO_2 group in the benzisoxazole ring results in its accommodation 0.10 nm more externally and 50° more distorted in the CPC (compared to 6-NitroCBI), a condition that justifies its smallest stabilization energy among the four systems (see Table 2). The expressive fluctuation in *P*3 parameter indicates high interaction dynamics between COO^- and NMe_3^+ groups in the complexes, which corroborates with both the smallest EL and VDW energetic contributions as well as the largest number of HBs with the solvent (*P*5). The highest *P*5 value observed for 6-NitroCBI⊂P5A system was initially considered as a potential factor involved in its inhibitory effects, but its similarity with *P*5 value for the 5,6-DinitroCBI⊂P5A as well as the opposite kinetic behaviour (catalysis and inhibition) observed for these complexes suggested that more factors should be involved in these effects.

In order to explore additional factors involved mainly in the inhibitory kinetic effects the atomic charges (Table 4) and the electrostatic potentials (ELPs, Fig. S17, ESI†) of the studied CBI derivatives were calculated for all environments (H_2O and in the pillararenes cavities) using PCM method and the geometric structure of the complexes. During the single step of the CBI decarboxylation, the O–N bond cleavage (from isoxazole ring) occurs with gain of electronic charge in the oxygen atom to form the corresponding cyanophenolate. Based on this premise and the calculated atomic charges the high polarization of the O–N bond in the 6-NitroCBI⊂P5A system proves to be an important factor involved in the inhibitory kinetic effects. In other words, the reduced ability of the oxygen atom to gain electronic charge in TS makes the reaction kinetically unfavorable.

The donor field effects already mentioned in the "^{1}H NMR titration" topic (promoted by the high electronic density from the P5A cavity on NO_2 group in the inhibitory system) was confirmed by the increasing in the electronic charges for both oxygen and nitrogen atoms of the NO_2 group. We also emphasize that these electronic effects can present a direct dependence on each other, for example, the high polarization of the O–N bond (from isoxazole ring) being influenced by the reduction of the electron withdrawing inductive effects of the NO_2 group. The considerations up to this point provide a broad perspective regarding the studied systems, with the simultaneous participation

Table 3 Five parameters calculated for the four complexes formed between CBI nitrated derivatives and cationic pillararenes

	P5A		P6A	
Parameter	6-NitroCBI	5,6-DinitroCBI	6-NitroCBI	5,6-DinitroCBI
*P*1	0.45 nm above	0.55 nm above	0.45 nm below	0.45 nm below
*P*2	15° insertion	65° insertion	15° insertion	15° insertion
*P*3	High fluctuation	High fluctuation	0.30 nm	0.31 nm
*P*4	−25 kJ mol^{-1} (EL)	−65 kJ mol^{-1} (EL)	−100 kJ mol^{-1} (EL)	−100 kJ mol^{-1} (EL)
	−130 kJ mol^{-1} (VDW)	−130 kJ mol^{-1} (VDW)	−165 kJ mol^{-1} (VDW)	−205 kJ mol^{-1} (VDW)
*P*5	Average = 5	Average = 4	Average = 2	Average = 2
	Max. = 8	Max. = 7	Max. = 5	Max. = 4

P1, average distance between C6 and the CPC; P2, spatial orientation/angle of the CBI derivative in the CPC measured between two longitudinal vectors (V_1 = aligned to the CPC; V_2 = formed by carbons C3 and C6 from CBI derivative); P3, average distance between charged groups (COO^- and NMe_3^+); P4, energetic contributions from EL and VDW interactions; P5, number of HBs between water and COO^- groups from CBI derivative.

Table 4 Atomic charges of the oxygen and nitrogen atoms (from the isoxazole ring and NO_2 groups) of the CBI nitrated derivatives in all environments (H_2O, P5A and P6A cavities)

	H_2O		P5A		P6A	
Atom/group	6-NitroCBI	5,6-DinitroCBI	6-NitroCBI	5,6-DinitroCBI	6-NitroCBI	5,6-DinitroCBI
O-Ring	−0.447	−0.452	−0.551	−0.436	−0.462	−0.436
N-Ring	−0.255	−0.225	−0.180	−0.232	−0.217	−0.212
5-NO_2	—	−0.379 (O)	—	−0.354 (O)	—	−0.371 (O)
		−0.402 (O′)		−0.358 (O′)		−0.361 (O′)
		0.364 (N)		0.207 (N)		0.178 (N)
6-NO_2	−0.420 (O)	−0.385 (O)	−0.446 (O)	−0.380 (O)	−0.409 (O)	−0.363 (O)
	−0.416 (O′)	−0.389 (O′)	−0.452 (O′)	−0.405 (O′)	−0.411 (O′)	−0.371 (O′)
	0.383 (N)	0.364 (N)	0.215 (N)	0.192 (N)	0.067 (N)	0.137 (N)

of steric and electrostatic effects naturally extending to larger discussions related to supramolecular and enzyme catalysis/inhibition.

4. Conclusions

In this work, experimental and theoretical studies about spontaneous hydrolysis and supramolecular kinetic effects by pillararenes on decarboxylation reaction of two CBI nitrated derivatives provided conclusive information about the components (CBIs and macrocycles) both individually and when in the complex. Despite that both CBI derivatives present similar transition states during spontaneous decarboxylation reaction, the additional NO_2 group in 5,6-DinitroCBI resulted in a lower energy barrier during its decomposition. In the presence of pillararenes both CBI derivatives complexed in H:G stoichiometries, being the particularity of each one in accommodating (geometry of complexes) the main determining factor between catalytic or inhibitory effects as well as the magnitude of rate and binding constants. Specifically, intrinsic effects involving the polarity modification of specific regions of the CBI derivatives, changes in the number of hydrogen bonds (between solvent and COO^- group from CBI) and field effects on NO_2 groups were the main factors responsible for the observed kinetic effects. Additionally, the effects observed on this model reaction stimulate new work and applications of pillararenes as supramolecular catalysts, functional group protectors in chemical reactions, chemical sensors, drug delivery and others. Finally, we envision that supramolecular and enzymatic catalytic processes can be fundamentally better represented considering the spatiotemporal and preorganization theories, with the postulates of both together providing greater deductive power than each one separately.

Author contributions

E. V. S. obtained and processed the kinetics and NMR data. The theoretical study was performed by R. M. (molecular dynamics) and L. S. (TSs and IRCs). V. N. performed the synthetic procedures. The manuscript was written by E. V. S. This work was supervised by L. G. R., M. M., F. N., R. F. A. and G. A. M. All authors have given approval to the final version of the manuscript.

Conflicts of interest

There are no conflicts to declare.

Acknowledgements

We dedicate this work on the memory of Professor Faruk Nome who passed away (September 24, 2018) during the preparation of this paper. His professional and personal efforts have made this possible. We thank Brazilian funding agencies CNPq, CAPES and FAPESC, Central de Análises (UFSC) for NMR analysis and CEBIME (UFSC) for HRMS/ESI-TOF analysis. RFA thanks CNPq/INCT-Catálise for financial support (grant 444061/2018-5) and FAPESC TO (no. 2019TR0847). LGR thanks

Ministerio de Economía y Competitividad of Spain (CTQ2017-84354-P), Xunta de Galicia (GR 2007/085; IN607C 2016/03) and Centro singular de investigación de Galicia accreditation (2016–2019, ED431G/09) and the European Union (European Regional Development Fund-ERDF). R. M. thanks Fondecyt (1171870). V. N. thank FAPERJ (E-26/202.911/2019) for financial support.

References

1 F. M. Menger and F. Nome, *ACS Chem. Biol.*, 2019, **14**, 1386–1392.
2 B. S. Souza, J. R. Mora, E. H. Wanderlind, R. M. Clementin, J. C. Gesser, H. D. Fiedler, F. Nome and F. M. Menger, *Angew. Chem., Int. Ed.*, 2017, **56**, 5345–5348.
3 G. Jindal and A. Warshel, *Proteins: Struct., Funct., Genet.*, 2017, **85**, 2157–2161.
4 S. H. Schneider and S. G. Boxer, *J. Phys. Chem. B*, 2016, **120**, 9672–9684.
5 H. Lehle, J. M. Kriegl, K. Nienhaus, P. Deng, S. Fengler and G. U. Nienhaus, *Biophys. J.*, 2005, **88**, 1978–1990.
6 Y. Wu and S. G. Boxer, *J. Am. Chem. Soc.*, 2016, **138**, 11890–11895.
7 C. Bohne, *Chem. Soc. Rev.*, 2014, **43**, 4037–4050.
8 L. A. Marchetti, L. K. Kumawat, N. Mao, J. C. Stephens and R. B. P. Elmes, *Chem*, 2019, **5**, 1398–1485.
9 D. G. Liz, A. M. Manfredi, M. Medeiros, R. Montecinos, B. Gómez-González, L. Garcia-Rio and F. Nome, *Chem. Commun.*, 2016, **52**, 3167–3170.
10 E. H. Wanderlind, D. G. Liz, A. P. Gerola, R. F. Affeldt, V. Nascimento, L. C. Bretanha, R. Montecinos, L. Garcia-Rio, H. D. Fiedler and F. Nome, *ACS Catal.*, 2018, **8**, 3343–3347.
11 M. Bojtár, J. Kozma, Z. Szakács, D. Hessz, M. Kubinyi and I. Bitter, *Sens. Actuators, B*, 2017, **248**, 305–310.
12 Y.-M. Zhang, J.-X. Su, Q. Li, W.-J. Qu, X. Zhu, Y.-L. Leng, S.-F. Xin, H. Yao, Q. Lin and T.-B. Wei, *Supramol. Chem.*, 2016, **29**, 411–416.
13 T. Zhou, N. Song, H. Yu and Y. W. Yang, *Langmuir*, 2015, **31**, 1454–1461.
14 M. M. Tian, D.-X. Chen, Y.-L. Sun, Y.-W. Yang and Q. Jia, *RSC Adv.*, 2013, **3**, 22111–22119.
15 R. R. Kothur, B. A. Patel and P. J. Cragg, *Chem. Commun.*, 2017, **53**, 9078–9080.
16 S. Pan, M. Ni, B. Mu, Q. Li, X.-Y. Hu, C. Lin, D. Chen and L. Wang, *Adv. Funct. Mater.*, 2015, **25**, 3571–3580.
17 I. Nierengarten, S. Guerra, M. Holler, J.-F. Nierengarten and R. Deschenaux, *Chem. Commun.*, 2012, **48**, 8072–8074.
18 R. Joseph, A. Naugolny, M. Feldman, I. M. Herzog, M. Fridman and Y. Cohen, *J. Am. Chem. Soc.*, 2016, **138**, 754–757.
19 D. Wu, Y. Li, J. Shen, Z. Tong, Q. Hu, L. Li and G. Yu, *Chem. Commun.*, 2018, **54**, 8198–8201.
20 J. Catalán, C. Díaz and F. García-Blanco, *J. Org. Chem.*, 2000, **65**, 3409–3415.
21 S. P. S. Chandra and A. C. Sharada, *Int. J. Innovative Pharm. Sci. Res.*, 2014, **5**, 1006–1010.
22 Y. Masuda, Y. Utsui, Y. Shiraishi, T. Karasawa, K. Yoshida and M. Shimizu, *Epilepsia*, 1979, **20**, 623–633.
23 N. Ashwini, M. Garg, C. D. Mohan, J. E. Fuchs, S. Rangappa, S. Anusha, T. R. Swaroop, K. S. Rakesh, D. Kanojia, V. Madan, A. Bender, H. P. Koeffler, Basappa and K. S. Rangappa, *Bioorg. Med. Chem.*, 2015, **23**, 6157–6165.
24 G. Zheng, T. Chen, X. Peng and S. Long, *J. Chem.*, 2015, **2015**, 1–5.
25 R. A. Shastri and J. S. Varudkar, *Indian J. Chem., Sect. B: Org. Chem. Incl. Med. Chem.*, 2009, **48B**, 1156–1160.
26 A. Nuhrich, M. Varache-Lembège, J. Vercauteren, R. Dokhan, P. Renard and G. Devaux, *Eur. J. Med. Chem.*, 1996, **31**, 957–964.
27 M. L. Casey, D. S. Kemp, K. G. Paul and D. D. Cox, *J. Org. Chem.*, 1973, **38**, 2294–2301.
28 D. S. Kemp and K. G. Paul, *J. Am. Chem. Soc.*, 1975, **97**, 7305–7312.
29 D. S. Kemp, D. D. Cox and K. G. Paul, *J. Am. Chem. Soc.*, 1975, **97**, 7312–7318.
30 L. Brinchi, P. Di Profio, R. Germani, L. Goracci, G. Savelli, N. D. Gillitt and C. A. Bunton, *Langmuir*, 2007, **23**, 436–442.
31 Y. Hu, K. N. Houk, K. Kikuchi, K. Hotta and D. Hilvert, *J. Am. Chem. Soc.*, 2004, **126**, 8197–8205.
32 J. J. Lee and W. T. Ford, *J. Org. Chem.*, 1993, **58**, 4070–4077.
33 P. Di Profio, R. Germani, G. Savelli, G. Cerichelli, N. Spreti and C. A. Bunton, *J. Chem. Soc., Perkin Trans. 2*, 1996, 1505–1509.
34 M. V. Scarpa, P. S. Araujo, S. Schreier, A. Sesso, A. G. Oliveira and H. Chaimovich, *Langmuir*, 2000, **16**, 993–999.
35 F. P. Schmidtchen and W. Germany, *J. Chem. Soc., Perkin Trans. 2*, 1986, 135–141.
36 P. K. Grzyska, P. G. Czyryca, J. Purcell and A. C. Hengge, *J. Am. Chem. Soc.*, 2003, **125**, 13106–13111.
37 J. Gao, *J. Am. Chem. Soc.*, 1995, **117**, 8600–8607.
38 H. Zipse, G. Apaydin and K. N. Houk, *J. Am. Chem. Soc.*, 1995, **117**, 8608–8617.
39 O. Acevedo and W. L. Jorgensen, *J. Am. Chem. Soc.*, 2005, **127**, 8829–8834.
40 O. Acevedo and W. L. Jorgensen, *Acc. Chem. Res.*, 2010, **43**, 142–151.
41 J. Turner, A. K. Soper and J. L. Finney, *Mol. Phys.*, 1992, **77**, 411–429.
42 E. J. Nilsson, V. Alfredsson, D. T. Bowron and K. J. Edler, *Phys. Chem. Chem. Phys.*, 2016, **18**, 11193–11201.
43 H. E. Wirth, *J. Phys. Chem.*, 1967, **71**, 2922–2929.
44 B. Gómez, V. Francisco, F. Fernández-Nieto, L. Garcia-Rio, M. Martín-Pastor, M. R. Paleo and F. J. Sardina, *Chem. – Eur. J.*, 2014, **20**, 12123–12132.
45 E. V. Silveira, V. Nascimento, E. H. Wanderlind, R. F. Affeldt, G. A. Micke, L. Garcia-Rio and F. Nome, *J. Org. Chem.*, 2019, **84**, 9684–9692.
46 Y. Zhao and D. G. Truhlar, *Theor. Chem. Acc.*, 2008, **120**, 215–241.
47 M. J. Frisch, G. W. Trucks, H. B. Schlegel, G. E. Scuseria, M. A. Robb, J. R. Cheeseman, G. Scalmani, V. Barone,

B. Mennucci, G. A. Petersson, H. Nakatsuji, M. Caricato, X. Li, H. P. Hratchian, A. F. Izmaylov, J. Bloino, G. Zheng, J. L. Sonnenberg, M. Hada, M. Ehara, K. Toyota, R. Fukuda, J. Hasegawa, M. Ishida, T. Nakajima, Y. Honda, O. Kitao, H. Nakai, T. Vreven, J. A. Jr. Montgomery, J. E. Peralta, F. Ogliaro, M. Bearpark, J. J. Heyd, E. Brothers, K. N. Kudin, V. N. Staroverov, R. Kobayashi, J. Normand, K. Raghavachari, A. Rendell, J. C. Burant, S. S. Iyengar, J. Tomasi, M. Cossi, N. Rega, J. M. Millam, M. Klene, J. E. Knox, J. B. Cross, V. Bakken, C. Adamo, J. Jaramillo, R. Gomperts, R. E. Stratmann, O. Yazyev, A. J. Austin, R. Cammi, C. Pomelli, J. W. Ochterski, R. L. Martin, K. Morokuma, V. G. Zakrzewski, G. A. Voth, P. Salvador, J. J. Dannenberg, S. Dapprich, A. D. Daniels, Ö. Farkas, J. B. Foresman, J. V. Ortiz, J. Cioslowski and D. J. Fox, *Gaussian*, Gaussian Inc., Wallingford CT, 2009.

48 A. V. Marenich, C. J. Cramer and D. G. Truhlar, *J. Phys. Chem. B*, 2009, **113**, 6378–6396.

49 S. Pronk, S. Páll, R. Schulz, P. Larsson, P. Bjelkmar, R. Apostolov, M. R. Shirts, J. C. Smith, P. M. Kasson, D. Van Der Spoel, B. Hess and E. Lindahl, *Bioinformatics*, 2013, **29**, 845–854.

50 N. Schmid, A. P. Eichenberger, A. Choutko, S. Riniker, M. Winger, A. E. Mark and W. F. Van Gunsteren, *Eur. Biophys. J.*, 2011, **40**, 843–856.

51 H. J. C. Berendsen, J. R. Grigera and T. P. Straatsma, *J. Phys. Chem.*, 1987, **91**, 6269–6271.

52 H. J. C. Berendsen, J. P. M. Postma, W. F. Van Gunsteren, A. DiNola and J. R. Haak, *J. Chem. Phys.*, 1984, **81**, 3684–3690.

53 T. Darden, D. York and L. Pedersen, *J. Chem. Phys.*, 1993, **98**, 10089–10092.

